Inorg. Chem. **2006**, *45*, 9281–9289

Effect of the Environment on Molecular Properties: Synthesis, Structure, and Photoluminescence of Cu(I) Bis(2,9-dimethyl-1,10-phenanthroline) Nanoclusters in Eight Different Supramolecular Frameworks

Shao-Liang Zheng,* Milan Gembicky, Marc Messerschmidt, Paulina M. Dominiak, and Philip Coppens*

Department of Chemistry, State University of New York at Buffalo, Buffalo, New York 14260-3000

Received June 1, 2006

By selection of different charge-balancing anionic frameworks and different host-to-guest ratios, the photosensitizer-dye cation $[Cu(dmp)_2]^+$ (dmp = 2,9-dimethyl-1,10-phenanthroline) has been embedded in a series of three-dimensional host structures. It occurs with variable geometry in different states of aggregation, including weakly interacting monomers, isolated dimers, columns, and layers. A large variation in its emission lifetime is correlated with the relative energy level spacings of the guest- and host-framework components. In a fully saturated host framework, the lifetime exceeds values reported for a series of conventional $Cu(dmp)_2$ salts.

Introduction

Supramolecular solids are of considerable interest because of their potential applications, including separation, catalysis, storage of sensitive compounds, and opto-magnetic materials.[1] They provide a well-defined environment that can be varied by crystal engineering and thus offer an attractive possibility to dilute and isolate molecular species in different but periodic matrixes.[2−4] Yet, the photophysical and chemical properties of molecules embedded in supramolecular cavities have so far received scant attention. Differences in the guest molecule's aggregation and the geometry of its ground and excited states occur, which can be studied by conventional and time-resolved diffraction methods.[5,6]

In preceding papers, we described a series of supramolecular solids encapsulating photoactive guest molecules, such as benzophenone,[7] benzil,[3,8] and xanthone,[4] which exhibit pronounced variations of molecular conformation. A joint structural, theoretical, and photophysical analysis verified that the relative energy level spacings of the guest and the host components play a crucial role in intermolecular energy transfer in the supramolecular solids and the resulting luminescence quenching.[9]

Because of the first emission and emission quenching studies of the $[Cu(dmp)_2]^+$ (dmp = 2,9-dimethyl-1,10-phenanthroline) cation at room temperature in solution by McMillin et al. in 1980,[10] the photochemistry and photophysics of this and related systems have received extensive attention.[11] Our previous work has shown that in a series of neat crystals the emission lifetimes of the $[Cu(diimine)_2]^+$

* To whom correspondence should be addressed. E-mail: coppens@buffalo.edu (P.C.), szheng4@buffalo.edu (S.-L.Z.).

(1) See for example: (a) *Host−Guest-Systems Based on Nanoporous Crystals*; Laeri, F., Schuth, F., Simon, U., Wark, M., Eds.; John Wiley & Sons: New York, 2003. (b) *Separations and Reactions in Organic Supramolecular Chemistry*; Toda, F., Bishop, R., Eds.; John Wiley & Sons: New York, 2004. (c) Holman, K. T.; Pivovar, A. M.; Swift, J. A.; Ward, M. D. *Acc. Chem. Res.* **2001**, *34*, 107−118. (d) Rowsell, J. L. C.; Yaghi, O. M. *Angew. Chem.*, Int. Ed. **2005**, *44*, 4670−4679.
(2) Coppens, P.; Ma, B.-Q.; Gerlits, O.; Zhang, Y.; Kulshrestha, P. *CrystEngComm.* **2002**, 302−309.
(3) (a) Ma, B.-Q.; Vieira Ferreira, L. F.; Coppens, P. *Org. Lett.* **2004**, *6*, 1087−1090. (b) Zheng, S.-L.; Coppens, P. *CrystEngComm.* **2005**, 289−293.
(4) Zheng, S.-L.; Coppens, P. *Chem.—Eur. J.* **2005**, *11*, 3583−3590.
(5) (a) Coppens, P.; Novozhilova, I. V. *Faraday Discuss.* **2003**, *122*, 1−11. (b) Coppens, P. *Chem. Commun.* **2003**, 1317−1320. (c) Coppens, P.; Vorontsov, I. I.; Graber, T.; Gembicky, M.; Kovalevsky, A. Yu. *Acta Crystallogr., Sect. A* **2005**, *61*, 162−172.
(6) (a) Coppens, P.; Vorontsov, I. I.; Graber, T.; Kovalevsky, A. Yu.; Chen, Y.-S.; Wu, G.; Gembicky, M.; Novozhilova, I. V. *J. Am. Chem. Soc.* **2004**, *126*, 5980−5981. (b) Coppens, P.; Gerlits, O.; Vorontsov, I. I.; Kovalevsky, A. Yu.; Chen, Y.-S.; Graber, T.; Novozhilova, I. V. *Chem. Commun.* **2004**, 2144−2145. (c) Vorontsov, I. I.; Kovalevsky, A. Yu.; Chen, Y.-S.; Graber, T.; Novozhilova, I. V.; Omary, M. A.; Coppens, P. *Phys. Rev. Lett.* **2005**, *94*, 193003.
(7) Ma, B.-Q.; Coppens, P. *Crys. Growth Des.* **2004**, *4*, 1377−1385.
(8) Ma, B.-Q.; Zhang, Y.-G.; Coppens, P. *J. Org. Chem.* **2003**, *68*, 9467−9472.
(9) Zheng, S.-L. Coppens, P. *Crys. Growth Des.* **2005**, *5*, 2050−2059.
(10) Blaskie, M. W.; McMillin, D. R. *Inorg. Chem.* **1980**, *19*, 3519−3522.
(11) Scaltrito, D. V.; Thompson, D. W.; O'Callaghan, J. A.; Meyer, G. J. *Coord. Chem. Rev.* **2000**, *208*, 243−266.

10.1021/ic0609709 CCC: $33.50
Published on Web 10/18/2006

Scheme 1. Structures of (a) CMCR, CECR, (b) THPM, THPE, (c) THPiPB, (d) THPB, and (e) CHTA

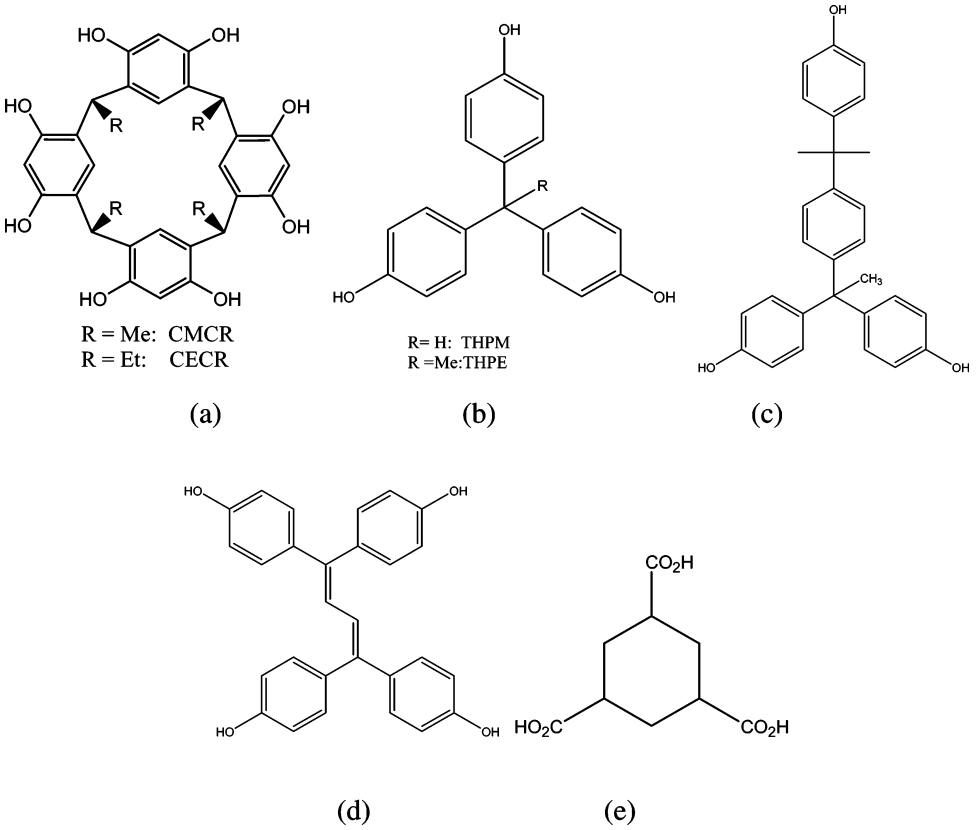

(diimine = substituted 1,10-phenanthroline) cations vary with the counterion.[12,13] In the current work, we describe the trapping and dilution of $[Cu(dmp)_2]^+$ in eight different anionic frameworks formed by resorcinerenes, poly(hydroxyphenyl) compounds, and fully saturated cyclohexanetricarboxylic acid. They have the composition $[Cu(dmp)_2][(CECR)^--2H_2O]-$benzene (**1**), $[Cu(dmp)_2][(CMCR)^--2H_2O]-$benzene (**2**), $[Cu(dmp)_2][(THPM)^-]$ (**3**), $[Cu(dmp)_2][(THPE)^-]$ (**4**), $[Cu(dmp)_2][(THPiPB)^-]$ (**5**), $[Cu(dmp)_2][(2THPE)^-]-H_2O$ (**6**), $[Cu(dmp)_2][(THPB)^-]$ (**7**), and $[Cu(dmp)_2][(CHTA)^-]-$EtOH (**8**) (CECR = *C*-ethylcalix[4]resorcinarene, CMCR = *C*-methylcalix[4]resorcinarene, THPM = tris(4-hydroxyphenyl)methane, THPE = tris(4-hydroxyphenyl)ethane, THPiPB = α,α,α′-tris(4-hydroxyphenyl)-1-ethyl-4-isopropylbenzene, THPB = 1,1,4,4-tetrakis(4-hydroxyphenyl)buta-1,3-diene, and CHTA = 1,3,5-cyclohexanetricarboxylic acid, Scheme 1). The synthetic strategies used and the structures and photophysical properties of the new phases are discussed below.

Experimental Section

Synthesis. All compounds were prepared by hydrothermal synthesis by sealing the reactants in a 6 mL tube and heating in an oven to the temperatures specified below. Only for complexes **4**−**7** was sufficient material produced by hydrothermal synthesis to allow microanalysis.

$[Cu(dmp)_2][(CECR)^--2H_2O]-$Benzene (1). Reactants included freshly prepared $Cu(OH)_2$ (0.5 mmol), CECR (0.5 mmol), NaOH (0.5 mmol), water (2 mL), and benzene (1 mL). The tube was allowed to stay at 160 °C for 48 h, followed by cooling to room temperature over 60 h. Red crystals appeared during the cooling period.

Synthesis of $[Cu(dmp)_2][(CMCR)^--2H_2O]-$Benzene (2). The preparation was identical to that for **1**, with CECR replaced by CMCR.

Synthesis of $[Cu(dmp)_2][(THPM)^-]$ (3). Reactants included freshly prepared $Cu(OH)_2$ (0.5 mmol), THPM (0.5 mmol), NaOH (0.5 mmol), and water (3 mL). The tube was allowed to stay at 120 °C for 30 h, followed by cooling to room temperature over 48 h. Red crystals appeared during the cooling period.

Synthesis of $[Cu(dmp)_2][(THPE)^-]$ (4). Reactants included freshly prepared $Cu(OH)_2$ (0.5 mmol), THPE (0.5 mmol), NaOH (0.5 mmol), and water (3 mL). The tube was allowed to stay at 160 °C for 48 h, followed by cooling to room temperature over 60 h. Red crystals appeared during the cooling period. Anal. Calcd for **4** ($C_{48}H_{41}CuN_4O_3$): C, 73.40; H, 5.26; N, 7.13. Found: C, 73.07; H, 5.32; N, 7.06.

Synthesis of $[Cu(dmp)_2][(THPiPB)^-]$ (5). Reactants included freshly prepared $Cu(OH)_2$ (0.5 mmol), THPiPB (0.5 mmol), NaOH (0.5 mmol), and water (3 mL). The tube was allowed to stay at 140 °C for 36 h, followed by cooling to room temperature over 48 h. Red crystals appeared during the cooling period. Anal. Calcd for **5** ($C_{57}H_{51}CuN_4O_3$): C, 75.77; H, 5.69; N, 6.20. Found: C, 75.77; H, 5.58; N, 5.82.

Synthesis of $[Cu(dmp)_2][(2THPE)^-]-2H_2O$ (6). The preparation was identical to that for **4**, with 1.0 mmol of THPE instead of 0.5 mmol. Anal. Calcd for **6** ($C_{68}H_{61}CuN_4O_7$): C, 73.59; H, 5.54; N, 5.05. Found: C, 73.15; H, 5.79; N, 5.42.

(12) Kovalevsky, A. Yu.; Gembicky, M.; Novozhilova, I. V.; Coppens, P. *Inorg. Chem.* **2003**, *42*, 8794−8802.
(13) Kovalevsky, A. Yu.; Gembicky, M.; Coppens, P. *Inorg. Chem.* **2004**, *43*, 8282−8289.

Table 1. Crystal Data and Structure Refinement of **1**−**8**

	1	**2**	**3**	**4**
empirical formula	$C_{67}H_{70}CuN_4O_{10}$	$C_{66}H_{65}CuN_4O_{10}$	$C_{47}H_{39}CuN_4O_3$	$C_{48}H_{41}CuN_4O_3$
fw	1154.82	1137.76	771.36	785.39
crystal system	monoclinic	triclinic	monoclinic	monoclinic
space group	$P2_1/c$ (No. 14)	$P\bar{1}$(no. 2)	$C2/c$ (no. 15)	$P2_1/c$ (no. 14)
		$A\bar{1}$		
a (Å)	13.049(1)	12.866(1)	37.340(1)[a]	14.890(2)
		12.866		
b (Å)	21.570(1)	14.490(1)	10.621(1)	17.595(2)
		21.193		
c (Å)	22.153(1)	15.224(1)	25.553(1)	20.016(2)
		20.840		
α (Å)	90	89.038(2)	90	90
		92.832		
β (Å)	108.581(3)	83.673(2)	129.339(1)	131.779(6)
		97.702		
χ (Å)	90	85.586(2)	90	90
		88.479		
V (Å^3)	5910.1(5)	2812.3(3)	7837.7(4)	3910.5(8)
		5624.6		
Z	4	2	8	4
		4		
μ (Mo Kα)/mm^{-1}	0.433	0.454	0.604	0.607
reflections collected	67736	23443	41947	57867
independent reflections	16576	10883	9976	9368
R_{int}	0.0309	0.0281	0.0215	0.0317
GOF on F^2	1.033	1.125	1.031	1.028
R_1 [$I > 2\sigma(I)$]	0.0579	0.0624	0.0368	0.0363
wR_2 (all data)	0.1764	0.1636	0.1066	0.1091
$\Delta\rho_{max}/\Delta\rho_{min}$ (e Å^{-3})	1.156/−0.766	1.641/−0.643	0.541/−0.453	1.497/−0.526

	5	**6**	**7**	**8**
empirical formula	$C_{57}H_{51}CuN_4O_3$	$C_{68}H_{61}CuN_4O_7$	$C_{56}H_{45}CuN_4O_4$	$C_{39}H_{41}CuN_4O_7$
fw	903.56	1109.75	901.50	741.30
crystal system	monoclinic	monoclinic	monoclinic	monoclinic
space group	$P2_1/c$ (no. 14)	$P2_1/c$ (no. 14)	$P2_1/c$ (no. 14)	Cc (no. 9)
a (Å)	9.827(1)	11.918(1)	11.059(1)	17.893(1)
b (Å)	33.132(1)	20.779(1)	18.842(1)	18.539(1)
c (Å)	14.180(1)	23.921(1)	23.524(1)	12.455(1)
β (Å)	103.593(1)	111.663(1)	113.631(1)	120.122(1)
V (Å^3)	4487.5(3)	5505.6(3)	4490.9(2)	3573.8(3)
Z	4	4	4	4
μ (Mo Kα)/mm^{-1}	1.337	1.339	0.540	0.667
reflections collected	60016	86190	48606	22176
independent reflections	13699	13674	12611	6995
R_{int}	0.0298	0.0238	0.0360	0.0196
GOF on F^2	1.089	1.037	1.024	1.038
R_1 [$I > 2\sigma(I)$]	0.0538	0.0440	0.0487	0.0654
wR_2 (all data)	0.1389	0.1265	0.1404	0.1623
$\Delta\rho_{max}/\Delta\rho_{min}$ (e Å^{-3})	1.610/−0.888	0.700/−0.467	0.871/−0.819	1.343/−0.781

[a] Represents an alternative nonprimitive cell to illustrate the similarity with **1** (transformation matrix: (1, 0, 0; 0, −1, 1; 0, −1, −1)).

Synthesis of [Cu(dmp)$_2$][(THPB)$^-$] (7). The preparation was identical to that for **3**, with THPM replaced by THPB. Anal. Calcd for **7** ($C_{56}H_{45}CuN_4O_4$): C, 74.60; H, 5.03; N, 6.21. Found: C, 74.17; H, 5.18; N, 6.10.

Synthesis of [Cu(dmp)$_2$][(CHTA)$^-$]−EtOH (8). Reactants included freshly prepared $Cu(OH)_2$ (0.5 mmol), CHTA (0.5 mmol), NaOH (0.5 mmol), toluene (2 mL), and EtOH (1 mL). The tube was allowed to stay at 100 °C for 24 h, followed by cooling to room temperature over 30 h. Orange-red crystals appeared during the cooling period.

X-ray Crystallography. Diffraction data for **1**−**8** were collected at 90 K on a Bruker APEXII charge-coupled device (CCD) diffractometer (Mo Kα, $\lambda = 0.71073$ Å). The data were integrated, scaled, sorted, and averaged using the SMART software package.[14] The structures were solved with direct methods and refined with full-matrix least-squares using the SHELXTL program package.[15] Anisotropic thermal parameters were applied to all non-hydrogen atoms. Hydrogen atoms were generated at idealized positions. The hydroxyl OH hydrogens were refined starting from their positions in the difference maps. Crystal data as well as details of data collection and refinement are summarized in Table 1, and hydrogen bond parameters are listed in Table S1. Drawings were produced with Weblab Viewer Pro. 4.0.[16] Atomic displacement probability ellipsoid drawings of all structures are shown in Figure S1. Full details can be found in CCDC-292225-292231, 274074, which can be obtained free of charge via http://www.ccdc.cam.ac.uk/conts/retrieving.html or deposit@ccdc.cam.uk (the Cambridge Crystallographic Data Center, 12 Union Road, Cambridge CB2 1EZ, U.K.; fax: (+44) 1223-336-033).

(14) SMART and SAINTPLUS: Area Detector Control and Integration Software. Madison, WI, 2004.

(15) Sheldrick, G. M. SHELXTL 6.10, Program for Crystal Structure Determination. Madison, Wisconsin, 2000.

(16) *Weblab Viewer Pro. 4.0*; Molecular Simulations Inc.: San Diego, CA, 1997.

Theoretical Calculations. Time-dependent density functional theory (TD-DFT) calculations were performed with the B3LYP functional and the 6-31G** basis set employing the Gaussian03 suite of programs.[17] Starting with the X-ray geometries, the structures were optimized by energy minimization.

UV−Vis Reflectance and Photoluminescence Spectroscopy. UV−vis absorption measurements were made on a Perkin-Elmer Lambda 35 UV−vis spectrometer equipped with an integrating sphere for diffuse reflectance spectroscopy. The spectra were collected at room temperature in the 210−800 nm range. Powdered crystals homogeneously diluted with nonabsorbing MgO and gently tapped into a sample holder were used as samples.

Photoluminescence measurements were carried out on a home-assembled emission detection system. Samples consisting of several small single crystals were mounted on a copper pin attached to a DISPLEX refrigerator. A metallic vacuum chamber with quartz windows attached to the cryostat was evacuated to approximately 10^{-7} bar with a turbomolecular pump. The crystals were irradiated at 90 K with 366 nm light from a pulsed N_2-dye laser. The emitted light was collected by an Oriel 77348 PMT device, positioned at 90° to the incident laser beam, and processed by a LeCroy Digital Oscilloscope with a 1−4 GHz sampling rate.

Results and Discussion

Synthesis Strategy and Crystal Structure. The self-assembly of supramolecular frameworks is influenced by a number of factors, which include the solvent(s) used, the template, the stoichiometric ratio, the pH of the solution, and steric requirements of the framework structure.[9,18] Although the resorcinarenes, such as CMCR and CECR, are versatile building blocks that can generate a remarkable variety of different frameworks with bipyridyl-type spacers,[7,8,19] only a few examples of *two*-component complexes incorporating large guest molecules are known,[4] and very few anionic hydrogen-bonded frameworks have been described. We find that under hydrothermal conditions (i.e., 100−160 °C, 2−4 days, and pH 8−9), tris(hydroxyphenyl) compounds, such as THPE (Scheme 1b), can form anionic hydrogen-bonded frameworks when combined with a cation[20] and that careful choice of reaction conditions allows incorporation of large metallorganic cations.

Resorcinarene-Based Frameworks. The $(CECR)^-$ anions (Scheme 1a) in **1** adopt the bowl-shaped (*r-cis-cis-cis*) conformation with four intramolecular hydrogen bonds along their upper rim [O···O = 2.531(2)−2.846(2) Å, Table S1]. Adjacent anions are oriented in an up-and-down fashion and are connected by intermolecular hydrogen bonds [O···O = 2.461(2) Å], resulting in a chain along the *c* axis, which extends into wavelike layers parallel to the (010) plane via hydrogen bonding with two water molecules [O···O = 2.628(3)−2.921(2) Å, Figure 1]. Adjacent hydrogen-bonded layers are juxtaposed along the *b* axis. The bowl-shaped hollows of adjacent layers combine into nanosized cavities with a 10.7 × 13.0 × 22.1 Å effective cross-section, occupying 53.6% of the crystal volume.[21] A $[Cu(dmp)_2]^+$ [Cu−N = 2.001(2)−2.043(2) Å, N−Cu−N = 116.50(7)−128.60(7)°] cation and its center-of-symmetry related equivalent (symmetry code: $-x$, $-y$, $1 - z$) form well-defined dimers embedded in each cavity. Two adjacent phenanthroline rings interact by off-set intermolecular $\pi-\pi$ interactions with an interplanar distance of 3.45 Å (Figure 2a,b). No strong intermolecular interactions occur between adjacent dimeric $[Cu(dmp)_2]^+$ clusters or between the dimer and the host framework (Figures 1a and S2). Each cavity also contains a benzene molecule that fills a void left by the cations.

Replacement of CECR by CMCR gives compound **2**, with very similar two-dimensional hydrogen-bonded layers of host molecules parallel to the (011) plane (Figures 3 and S3).

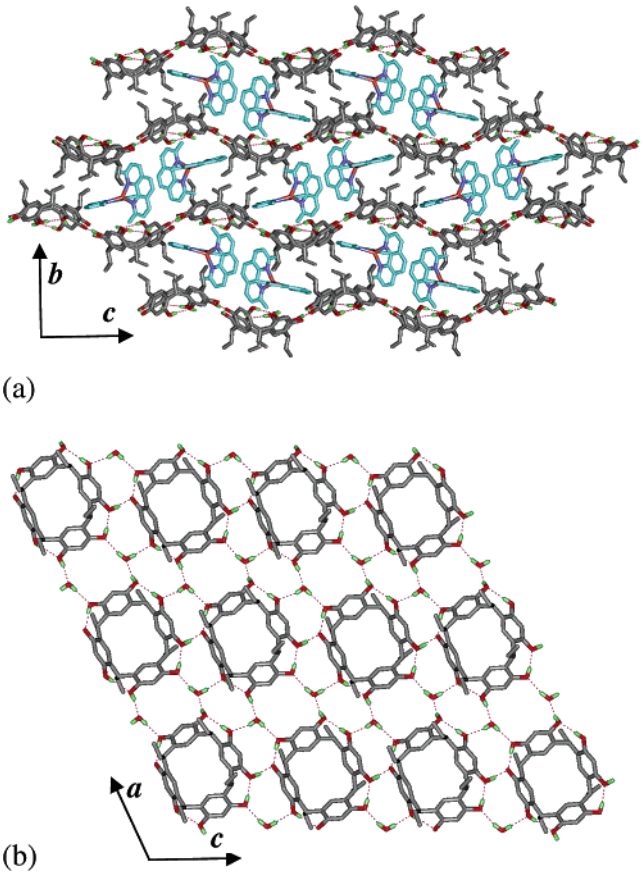

Figure 1. (a) Three-dimensional supramolecular array in **1** viewed along the *a*-axis direction (*c*-axis horizontal) and (b) top view (along *b*) of the two-dimensional hydrogen-bonded anionic layer (*c*-axis horizontal).

(17) Frisch, M. J.; Trucks, G. W.; Schlegel, H. B.; Scuseria, G. E.; Robb, M. A.; Cheeseman, J. R.; Zakrzewski, V. G.; Montgomery, J. A., Jr.; Stratmann, R. E.; Burant, J. C.; Dapprich, S.; Millam, J. M.; Daniels, A. D.; Kudin, K. N.; Strain, M. C.; Farkas, O.; Tomasi, J.; Barone, V.; Cossi, M.; Cammi, R.; Mennucci, B.; Pomelli, C.; Adamo, C.; Clifford, S.; Ochterski, J.; Petersson, G. A.; Ayala, P. Y.; Cui, Q.; Morokuma, K.; Malick, D. K.; Rabuck, A. D.; Raghavachari, K.; Foresman, J. B.; Cioslowski, J.; Ortiz, J. V.; Stefanov, B. B.; Liu, G.; Liashenko, A.; Piskorz, P.; Komaromi, I.; Gomperts, R.; Martin, R. L. D.; Fox, J.; Keith, T.; Al-Laham, M. A.; Peng, C. Y.; Nanayakkara, A.; Gonzalez, C.; Challacombe, M.; Gill, P. M. W.; Johnson, B.; Chen, W.; Wong, M. W.; Andres, J. L.; Gonzalez, C.; Head-Gordon, M.; Replogle, E. S.; Pople, J. A. *GAUSSIAN03*, revision C.02; Gaussian, Inc.: Pittsburgh, PA, 2003.

(18) See for example: (a) Moulton, B.; Zaworotko, M. J. *Chem. Rev.* **2001**, *101*, 1629−1658. (b) Zheng, S.-L.; Tong, M.-L.; Chen, X.-M. *Coord. Chem. Rev.* **2003**, *246*, 185−202. (c) Zheng, S.-L.; Yang, J.-H.; Yu, X.-L.; Chen, X.-M.; Wong, W.-T. *Inorg. Chem.* **2004**, *43*, 830−838.

(19) See for example: (a) MacGillivray, L. R.; Holman, K. T.; Atwood, J. L. *J. Supramol. Chem.* **2001**, *1*, 125. (b) MacGillivray, L. R.; Reid, J. L.; Ripmeester, J. A. *Chem. Commun.* **2001**, 1034−1035.

(20) Zheng, S.-L.; Messerschmidt, M.; Coppens, P. *Angew. Chem.*, Int. Ed. **2005**, *44*, 4614−4617.

(21) Spek, A. L. *PLATON, A Multipurpose Crystallographic Tool*; Untrecht University: Utrecht, The Netherlands, 2003.

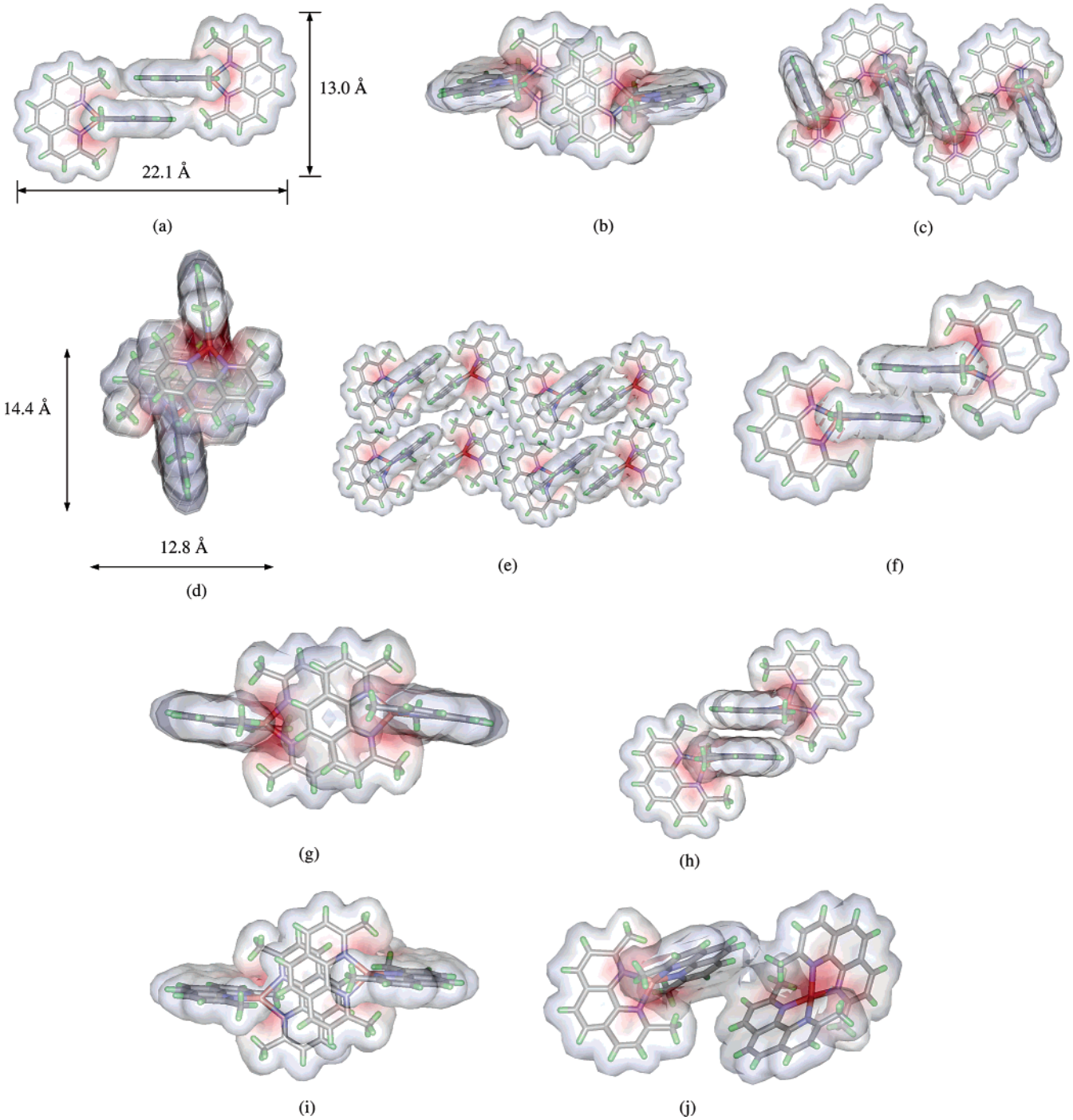

Figure 2. (a) Side view and (b) top view of the nanosized dimeric $[Cu(dmp)_2]^+$ cations connected by $\pi-\pi$ interactions in **1**, (c) side view and (d) top view of the nanosized $[Cu(dmp)_2]^+$ column in **2**, (e) top view of the $[Cu(dmp)_2]^+$ layer in **3**, (f) side view and (g) top view of the dimeric $[Cu(dmp)_2]^+$ cations in **5**, (h) side view and (i) top view of the dimeric $[Cu(dmp)_2]^+$ cations in **6**, and (j) side view of the weakly interacting $[Cu(dmp)_2]^+$ monomers in **8**.

The similarity between the two structures is illustrated by the transformation of the triclinic unit cell of **2** to a cell centered in the A face, which leads to cell dimensions almost identical to those of **1** (column **2** of Table 1). Because of the smaller methyl tail of CMCR compared with CECR, the bowl-shaped cavities in each of the layers combine into channels parallel to the *a*-axis, with a volume corresponding to 57.5% of the crystal space. Thus, different from **1**, $[Cu(dmp)_2]^+$ cations [Cu−N = 2.018(3)−2.071(3) Å, N−Cu−N = 117.6(1)−140.3(1)°] form columns via $\pi-\pi$ (interplanar distance: 3.43 Å) and C−H···π interactions [(C−)H···π distance: 2.47 Å, Figure 2c,d] in each channel. The columns have a rectangular 14.4 × 12.8 Å cross-section and are well separated by the host framework. The channels contain one benzene molecule per unit cell, which fills a gap left by the cations.

Though the structures are very similar, the two-resorcinarene-based anionic framework contains the guest in different states of aggregation. Isolated dimeric $[Cu(dmp)_2]^+$ cations, such as that found in **1,** have not been observed before, even though a series of salts of $[Cu(dmp)_2]^+$ have been reported.[12]

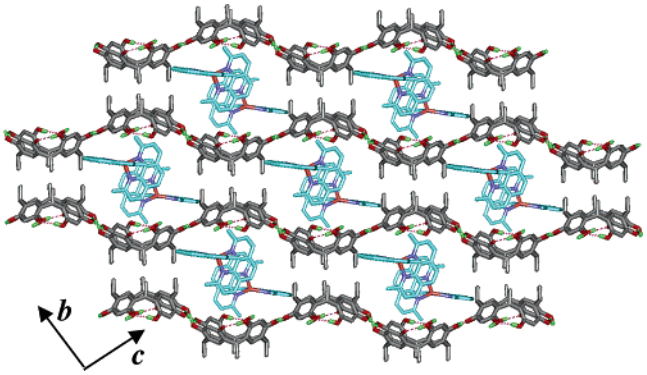

Figure 3. Three-dimensional supramolecular array in **2** viewed along the *a*-axis direction, which is the channel direction.

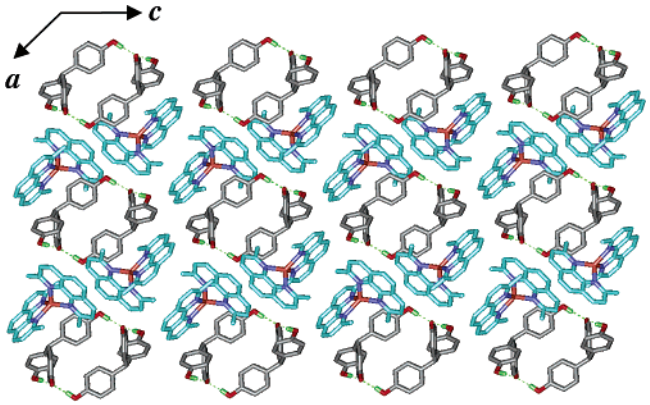

Figure 4. Three-dimensional supramolecular array in **3** viewed along the *b*-axis direction (*c*-axis horizontal).

Tris(hydroxyphenyl)-Based Frameworks. Similar to other T-shaped host molecules, such as 4,4-bis(4′-hydroxyphenyl)cyclohexanone,[22] the $(THPM)^-$ anion (Scheme 1b) in **3** is linked by hydrogen bonding to its symmetry-related equivalents [symmetry codes: $-x + 1/2, y - 1/2, -z + 3/2$ and $x, y - 1, z$; O···O 2.568(2) and 2.476(2) Å] to form a one-dimensional hydrogen-bonded anionic ladder parallel to [010] (Figures 4 and S4). Adjacent ladders are connected along [201] by van der Waals interactions, resulting in a two-dimensional supramolecular sheet of host molecules parallel to the $(10\bar{2})$ plane. Parallel sheets are at a distance of 9.3 Å, leaving a space accounting for 70.2% of the crystal volume, which contains cationic $[Cu(dmp)_2]^+$ layers [Cu−N = 2.023(1)−2.075(1) Å, N−Cu−N = 118.81(6)−138.82(5)°, Figure 2e]. The cations in the layers are connected by weak off-set $\pi-\pi$ (interplanar distance: 3.60 Å) and very weak C−H···π interactions [(C−)H···plane distance: 3.00 Å].

In **4**, $(THPM)^-$ is replaced by the $(THPE)^-$ anion (Scheme 1b). The structure features two-dimensional hydrogen-bonded layers of anions (Figures 5 and S5), linked by hydrogen bonding to their symmetry-related equivalents [symmetry codes: $x - 1, -y - 1/2, z - 1/2$ and $-x, y - 1/2, -z + 1/2$; O···O 2.525(2) and 2.491(2) Å], leading to a two-dimensional wavelike layer parallel to the $(10\bar{2})$ plane. As $(THPE)^-$ acts as a Y-shaped host molecule, the two-dimensional layers have an unusual (4.8^2) topological motif (Scheme S1).[23,24] Adjacent layers are juxtaposed so as to leave a space that contains $[Cu(dmp)_2]^+$ cations [Cu−N = 2.027(1)−2.039(1) Å, N−Cu−N = 118.78(5)−128.52(5)°] arranged in columns via $\pi-\pi$ (interplanar distance: 3.31 Å) and C−H···π interactions [(C−)H···plane distance: 2.55 Å] with a 9.6 × 20.0 Å effective cross-section.

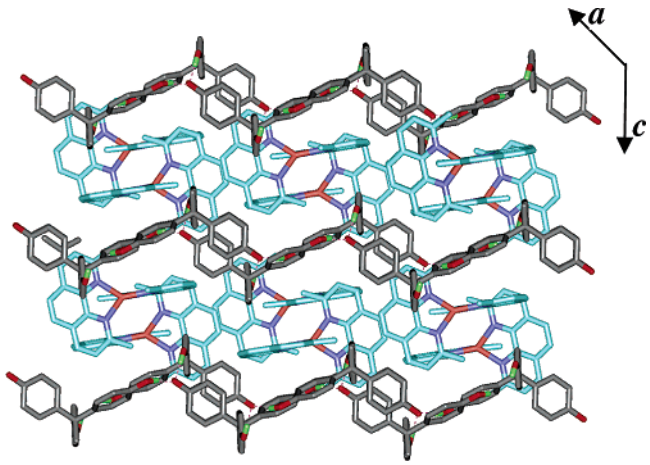

Figure 5. Three-dimensional supramolecular array in **4** viewed along the *b*-axis direction.

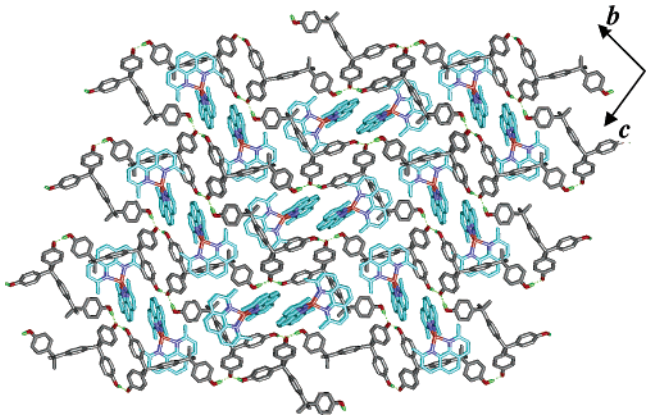

Figure 6. Three-dimensional supramolecular array in **5** viewed along the *a*-axis direction.

Replacement of THPE by THPiPB (Scheme 1c) gives **5**, which contains a similar two-dimensional wavelike hydrogen-bonded layer parallel to $(10\bar{2})$ (Figures 6 and S6). Adjacent layers are juxtaposed so as to leave large cavities with a 9.4 × 13.2 × 20.9 Å effective cross-section, accounting for 58.2% of the crystal volume. One of the branches of the THPiPB molecule is much longer than in THPE, which interferes with layer structure formation. As a result, a $[Cu(dmp)_2]^+$ cation [Cu−N = 2.005(2)−2.064(2) Å, N−Cu−N = 113.05(7)−139.40(7)°] and its center-of-symmetry related equivalent (symmetry code: $x, y, 1 - z$) are embedded in each channel as a dimer, as in **1**, the dimers being separated by the long branch of THPiPB. The face-to-face stacking

(22) Aitipamula, S.; Nangia, A. *Chem.—Eur. J.* **2005**, *11*, 6727−6742.

(23) (a) Delgado-Friedrichs, O.; O'Keeffe, M. *J. Solid State Chem.* **2005**, *178*, 2480−2485. (b) Dolomanov, O. V.; Blake, A. J.; Champness, N. R.; Schröder, M. *J. Appl. Crystallogr.* **2003**, *36*, 1283−1284. (c) Dolomanov, O. V. *OLEX*, version 2.55, 2004.

(24) See for example: (a) Long, D.-L.; Blake, A. J.; Champness, N. R.; Schröder, M. *Chem. Commun.* **2000**, 1369−1370. (b) Zheng, S.-L.; Tong, M.-L.; Zhu, H.-L.; Fang, Y.; Chen, X.-M. *J. Chem. Soc., Dalton Trans.* **2001**, 2049−2053.

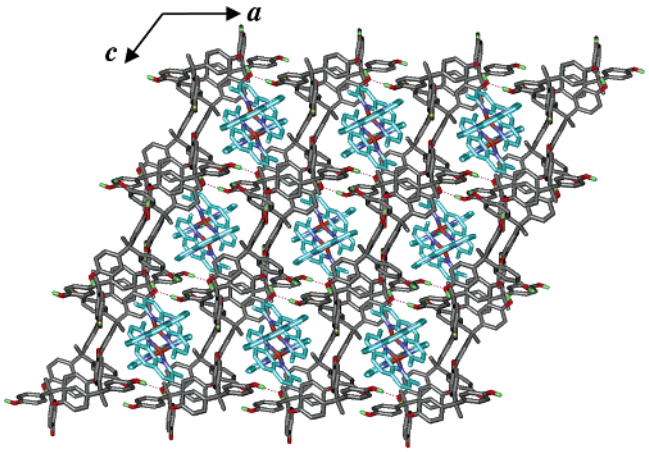

Figure 7. Three-dimensional network in **6** viewed along the *b*-axis direction (*a*-axis horizontal).

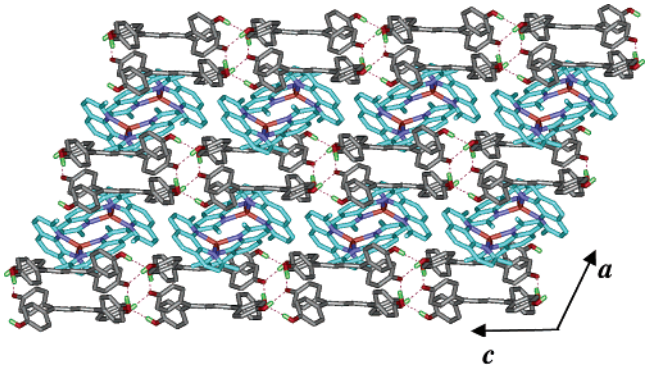

Figure 8. Three-dimensional supramolecular array in **7** viewed along the *b*-axis direction (*c*-axis horizontal).

distance of the aromatic rings, which are offset from each other, is 3.35 Å (Figure 2f,g).

Doubling the THPE-host-to-$[Cu(dmp)_2]^+$-guest ratio used for **4** yields **6** with completely embedded dimeric $[Cu(dmp)_2]^+$ cations. Two crystallographically independent THPE molecules share one hydrogen atom, with a short O···O distance [O(1)···O(5) = 2.485(2) Å], typical for acid salts. Adjacent $(2THPE)^-$ units are connected by intermolecular hydrogen bonds [O···O = 2.520(2)−2.772(2) Å], which extend into a three-dimensional hydrogen-bonded anionic framework [O···O 2.525(5)−2.528(5) Å] with large channels (effective dimension: 12.8 × 10.3 Å), constituting 50.3% of the crystal volume and running along the *b*-axis (Figures 7 and S7). In each channel, a $[Cu(dmp)_2]^+$ cation [Cu−N = 1.996(1)−2.068(2) Å, N−Cu−N = 106.01(6)−133.49(6)°] is connected with its center-of-symmetry related equivalent (symmetry code: $-x$, $1-y$, $1-z$) via $\pi-\pi$ interactions (interplanar distance: 3.63 Å, Figure 2h,i) to form an isolated dimer. One lattice water molecule is clathrated in each channel and hydrogen-bonded to the hydroxyl oxygen atom [O(1W)−H···O = 3.182(3) Å] of the host network.

Comparison with **4** confirms that supramolecular host matrixes can be manipulated by variation in the stoichiometric ratio, in this case leading to different states of guest aggregation.

Comparison of a Fully Conjugated and a Fully Saturated Framework. The 90 K lifetimes of the complexes

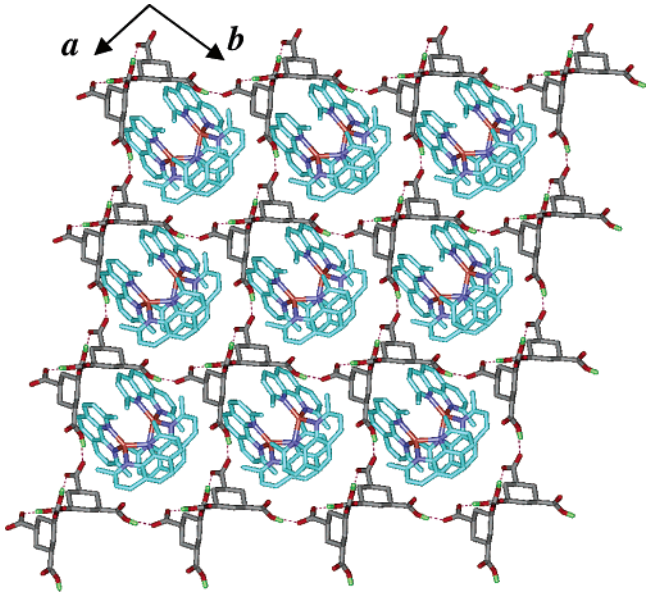

Figure 9. Three-dimensional network of in **8** viewed along the *c*-axis direction.

Table 2. Some Characteristics of $[Cu(dmp)_2]^+$ Inclusion Compounds

	host framework	states of guest aggregation	cavity/ one guest[a]	concn/ mol L^{-1}	RT	90 K
1	2-D layer	isolated dimer	727.5	1.123	371(9)	532(3)
2	2-D layer	column	663.0	1.181	348(5)	520(2)
3	1-D ladder	layer	687.5	1.696	286(9)	436(4)
4	2-D layer	column	671.7	1.699	310(4)	458(2)
5	2-D layer	isolated dimer	652.5	1.481	236(9)	357(4)
6	3-D network	isolated dimer	666.9	1.207	670(3)	1072(12)
7	2-D layer	layer	692.2	1.480	40(2)	60(2)
8	3-D network	weakly interacting monomer	620.5	1.859	1120(18)	2680(12)

[a] Solvent molecules excluded in calculation of cavity volume.

discussed so far are limited to ∼1 μs for **6** and 0.5 μs or less for **1**−**5**. To obtain more information on the relation between the lifetime and the nature of the framework, two new phases with a fully conjugate framework based on THPB[25] and a fully saturated framework based on CHTA[26] (Scheme 1d,e), respectively, were synthesized.

In **7**, the $(THPB)^-$ anion is linked by hydrogen bonding to its related equivalents [symmetry codes: x, $-y+1/2$, $z+1/2$; $-x$, $y+1/2$, $-z-1/2$; and x, $-y-1/2$, $z-1/2$; O···O 2.454(2) and 2.684(2) Å] to form a two-dimensional wavelike hydrogen-bonded layer parallel to the (100) plane (Figures 8 and S8). Adjacent layers are related by an *a*-axis translation so as to leave a layer-shaped space accounting for 61.7% of the crystal volume. Similar to **3**, the tris(4-hydroxyphenyl)methane inclusion compound, $[Cu(dmp)_2]^+$ ions [Cu−N = 2.018(2)−2.045(2) Å, N−Cu−N =

(25) Itami, K.; Ushiogi, Y.; Nokami, T.; Ohashi, Y.; Yoshida, J. *Org. Lett.* **2004**, *6*, 3695−3698.
(26) (a) Bhogala, B. R.; Vishweshwar, P.; Nangia, A. *Crys. Growth Des.* **2002**, *2*, 325−328. (b) Bhogala, B. R.; Nangia, A. *Crys. Growth Des.* **2003**, *3*, 547−554. (c) Bhogala, B. R.; Vishweshwar, P.; Nangia, A. *Crys. Growth Des.* **2005**, *5*, 1271−1281.

Table 3. Distortion of the Cu(I) Coordination for $[Cu(dmp)_2]^+$ Complexes

	1	2	3	4	5	6	7	8
rocking θ_x (deg)	86.98	100.88	99.04	89.08	84.88	74.46	87.8	97.26
wagging θ_y (deg)	92.63	98.21	97.80	95.90	79.49	97.59	90.01	87.17
flattening θ_z (deg)	97.94	97.05	96.90	92.65	101.55	98.72	103.47	92.67
Cu displacement	0.2105	0.2234	0.2712	0.0654	0.1869	0.4875	0.1462	0.0731
from dmp plane/Å	0.0250	0.1089	0.0588	0.0405	0.1931	0.0661	0.0012	0.0381

Table 4. Calculated Excited State Energy Separation of Anion Component in Different Inclusion Compound[a]

energy separation	$CECR^-$ *E*/eV (*f*)	$CMCR^-$ *E*/eV (*f*)	$THPM^-$ *E*/eV (*f*)	$THPE^-$ *E*/eV (*f*)	$THPiPB^-$ *E*/eV (*f*)	THPE[a] *E*/eV (*f*)	$THPB^-$ *E*/eV (*f*)	$CHTA^-$ *E*/eV (*f*)
S_0-T_1	2.884	2.574	1.802	1.847	1.405	3.666	1.162	3.778
	(0.000)	(0.000)	(0.000)	(0.000)	(0.000)	(0.000)	(0.000)	(0.000)
S_0-S_1	2.984	2.593	1.840	1.906	1.412	4.716	2.154	4.008
	(0.004)	(0.001)	(0.003)	(0.005)	(0.004)	(0.021)	(0.477)	(0.018)
S_0-S_2	3.340	2.994	2.239	2.293	1.837	4.905	2.453	4.019
	(0.024)	(0.004)	(0.021)	(0.012)	(0.002)	(0.035)	(0.001)	(0.005)

[a] For **6**, which contains $(2THPE)^-$, the gap was approximated by that for neutral THPE.

116.28(8)−133.11(7)°] are interspersed between the parallel layers, connected by off-set $\pi-\pi$ interactions (interplanar distance: 3.38 Å) and a weak C−H···π interaction [(C−)H···π distance: 2.93 Å].

In **8**, the $(CHTA)^-$ ions are linked by hydrogen bonding to their symmetry equivalents [symmetry codes: $x, -y, z - 1/2$ and $x - 1/2, -y + 1/2, z - 1/2$; O···O = 2.502(4) and 2.536(4) Å]. The molecule is essentially a four-connected node (Figures 9 and S9), which extends into a three-dimensional hydrogen-bonded anionic framework with 10^3 topology [O···O 2.497(5)−2.535(5) Å].[23] Weakly interacting monomers are located in channels (effective dimension: 12.8 × 10.3 Å) along the *c*-axis $[Cu(dmp)_2]^+$ [Cu−N = 1.932(3)−2.027(4) Å, N−Cu−N = 115.9(2)−128.5(2)°], which have a volume corresponding to 77.5% of the crystal space (Figure 2j). Unlike in **1**−**7**, no $\pi\cdots\pi$ interactions and only a weak C(sp^3)−H···π interaction [(C−)H···plane distance: 2.89 Å] are found between adjacent $[Cu(dmp)_2]^+$ cations. One ethanol molecule is clathrated in each channel and hydrogen-bonded to the hydroxyl oxygen atom [O(1S)−H···O = 2.822(6) Å] of the host network.

Nature of the $[Cu(dmp)_2]^+$ Cations. Most of the hosts examined form hydrogen-bonded layers between which the guest cations are interspersed. The exceptions are the 2:1 host/guest phase **6** with THPE, in which the excess host molecules form a three-dimensional framework; the tricarboxylic acid CHTA in **8**, which similarly is capable of forming a 3-D framework; and **3**, in which one-dimensional hydrogen-bonded ladders form sheets through van der Waals interactions. The guests are arranged in layers, channels, or cavities. Long side chains, as in **1** and **5**, lead to cavity formation.

The $[Cu(dmp)_2]^+$ cations occur in four different states of aggregation: isolated dimers, columns, layers of stacked molecules, and weakly interacting monomers (Figure 2, Table 2). The molecular distortions of the cation differ considerably in the series, as summarized in Table 3 and illustrated in Figure 10. Significant variation in the flattening, rocking, and wagging distortions (as defined in Scheme S2),[27] as well as in the Cu(I) displacement from the phenanthroline plane, occur. This is even the case among isolated dimeric $[Cu(dmp)_2]^+$ complexes: **1** (Figure 2a,b), **5** (Figure 2f,g), and **6** (Figure 2h,i). There is no clear correlation between the distortion of Cu(I) coordination and the cavity size. Other factors, such as the cavity shape, nature of the intermolecular interactions, and the presence of solvent molecules in some cases, are clearly more important than the volume of the cavity the molecule is embedded in.

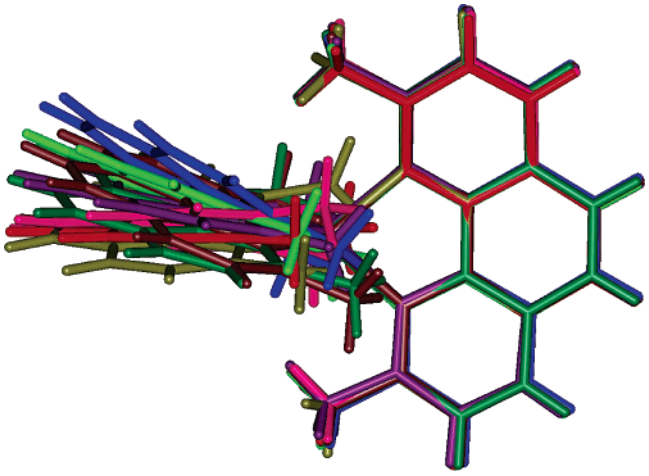

Figure 10. Diagram of superimposed $[Cu(dmp)_2]^+$ cations in **1** (red), **2** (brown), **3** (olive), **4** (dark yellow), **5** (green), **6** (blue), **7** (pink), and **8** (purple).

The concentration of the $[Cu(dmp)_2]^+$ guests in the structures surveyed is listed in column 5 of Table 2. It varies from 1.1 to almost 1.8 mol/L, which may be compared with concentrations of 2.5−2.6 mol/L in the more common PF_6^- and BF_4^- salts of $Cu(dmp)_2$.[12] Such dilution of photoactive molecules in periodic solids is of importance in time-resolved crystallographic studies, as, upon illumination, fewer photons are required to achieve a large excitation percentage of the photochemicaly active molecules.[2]

Spectroscopic Properties. Absoprtion spectra are shown in Figure S10. As in the neat $[Cu(dmp)_2]^+$ compounds,[12] the longest wavelength absorption band of **1**−**8** at ca. 450−550 nm can be assigned to the metal-to-ligand charge transfer (MLCT) transition of the Cu(I) cation. All complexes show

(27) Dobson, J. F.; Green, B. E.; Healy, P. C.; Kennard, C. H. L.; Pakawatchai, C.; While, A. H. *Aust. J. Chem.* **1984**, *37*, 649−659.

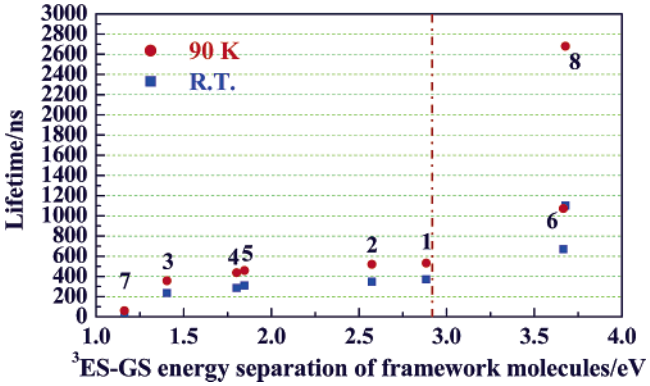

Figure 11. Relation between the excited-state lifetimes of **1**−**8** and the theoretical ^{3}ES−GS energy gaps of the anionic framework components. The vertical line represents the ^{3}ES−GS energy gap for the $[Cu(dmp)_2]^+$ ion (2.78 eV).[29] The increase in the lifetime of the embedded complexes beyond this value of the framework gap is evident. For **6**, which contains $(2THPE)^-$, the gap was approximated by that for neutral THPE.

strong orange-red emission with a broad, featureless profile in the 700−760 nm range. Lifetimes vary from (room temperature (RT)/90 K) 40/60 ns for **7** to 1120/2800 ns for **8**, with **1**−**5** being intermediate in the (RT/90 K) 236/357 ns (**3**) to 371/532 ns (**1**) range (Table 2).

As pointed out by Lower and El-Sayed in 1965,[28] luminescence quenching due to intermolecular energy transfer in the solid state will be much more pronounced for triplet than for singlet states. Our earlier analysis of the luminescence properties of supramolecular solids[9] shows that the energy transfer responsible for luminescence quenching in neutral guest−host systems correlates with the relative energy level spacings of the luminescing donor and quenching acceptor molecules. Examination of the excited state−ground state (^{3}ES−GS) energy gaps of the host molecules as calculated by TD-DFT (Table 4) confirms that a similar correlation exists for metallorganic cations embedded in an anionic host lattice, as illustrated in Figure 11.[29] The 1:2 THPE complex **6** (RT/90 K: 670/1072 ns) shows a much longer lifetime than the 1:1 complex with THPE (**4**) (RT/90 K: 310/458 ns). This difference is in the direction suggested by the larger excited state−ground state (^{3}ES−GS) energy gap of neutral THPE compared with $(THPE)^-$ (Table 4).

The lifetimes of the solids based on CECR, CMCR, and the fully anionic trihydroxyphenyl complexes are similar to each other in the 400−500 ns range (90 K). The outliers are the fully conjugated THPB salt (**7**) at 60 ns, the partially anionic THPE complex (**6**) (1072 ns), and especially the saturated cyclohexane−tricarboxylic acid-based solid (**8**) (2680 ns), with a longer lifetime at 90 K than that of any of the conventional $[Cu(dmp)_2]^+$ salts reported in ref 12 at 17 K. Not unexpectedly, the use of saturated frameworks leads to optimization of excited-state lifetimes of the guest molecules.

Concluding Remarks

In summary, $[Cu(dmp)_2]^+$ cations have been embedded in eight different supramolecular frameworks in different states of aggregation. As this is only a very small fraction of the supramolecular solids that can be synthesized, the versatility of the field is enormous. Different states of aggregation can be designed by only small variations in the framework components, such as the replacement of methyl by ethyl in the resorcinarenes. The photophysical properties of the new phases are strongly affected by the electronic structure of the framework components. Not unexpectedly, the use of saturated frameworks leads to optimization of excited-state lifetimes of the guest molecules. The short lifetime of $[Cu(dmp)_2]^+$ in the conjugated-host solid **7**, compared with the long lifetime in the fully saturated **8**, which exceeds that observed in a series of conventional $Cu(dmp)_2$ salts, is a prime manifestation of this effect. It follows that host−guest solids can be designed so as to optimize the desired photophysical properties.

The analysis described here and those reported elsewhere[4,9,30] serve as a guide for strategies to be adopted in the synthesis of long-lifetime luminescent materials.

Acknowledgment. We thank Dr. Irina Novozhilova for assistance with the TD-DFT calculations and Dr. Andrey Yu. Kovalesky for helpful discussions at the beginning of this work. The authors thank the U.S. Department of Energy for support of the spectroscopic experiments and theoretical calculations through grant DE-FG02-02ER15372. Support of this work by the National Science Foundation (CHE-0236317) and the Petroleum Research Fund of the American Chemical Society (PRF43594-AC4) is gratefully acknowledged.

Supporting Information Available: Additional plots and hydrogen bond tables (PDF), and X-ray data files (CIF). This material is available free of charge via the Internet at http://pubs.acs.org.

IC0609709

(28) Lower, S. K.; El-Sayed, M. A. *Chem. Rev.* **1966**, *66*, 199−241.
(29) For $[Cu(dmp)2]^+$, the ^{3}ES−GS energy gap is 2.78 eV; see: Chen, L. X.; Shaw, G. B.; Novozhilova, I.; Liu, T.; Jennings, G.; Attenkofer, K.; Meyer, G. J.; Coppens, P. *J. Am. Chem. Soc.* **2003**, *125*, 7022−7034.
(30) (a) Sudhakar, M.; Djurovich, P. I.; Hogen-Esch, T. E.; Thompson, M. E. *J. Am. Chem. Soc.* **2003**, *125*, 7796−7797. (b) Tanaka, I.; Tabata, Y.; Tokito, S. *Chem. Phys. Lett.* **2004**, *400*, 86−89.